AMERICAN JOURNALS
Open Access, Peer Reviewed Journals

American Journal of Technology and Applied Sciences
**ISSN (E): 2832-1766|** Volume 4, | Sep., 2022

# SYNTHESIS AND CHARACTERIZATION OF SrAl2O4: Eu, Dy NANOMATERIALS

**Victor Kadenge**
*University of Embu, Kenya Department of Physical Sciences*
*victorkadenge76@gmail.com*

***A B S T R A C T***

One purpose of this study is to describe current advances made mostly in preparation of luminescence nanoparticles based on a study that has been published. In outlining the benefits and limitations of various synthesis methods, we highlight recent advances on SrAl2O4: Eu, Dy nanoparticles. Such durable substance has various advantages over its precursors, including being more stable, efficient, and much less poisonous. Its design of an efficient synthesis process for SrAl2O4 dopant particles. As a result, the average particle size ranges between 20 and 100 micrometers. For contemporary usage that require semi nanoparticles, the high particle diameter is constraining. Its resulting luminescence emission is heavily influenced by the morphology and shape, which may be adjusted by modifying the control parameters. As a result, substantial effort like the sol-gel technique, hydrothermal synthesis, laser synthesis, combustion fabrication, and solid country reaction, has acquired quite a few interest as a result of this. A lot of those methods, even though, are incompatible to enormous production and sustainable requirements. strong synthesis values, in general between 1300 and 1900 °C, with prolonged processing instances are required in the industrial processing of distinctly crystalline powders, especially for strong kingdom reactions has gone into developing new ways for obtaining nanoparticles while minimizing time-consuming, difficult, expensive, or inefficient preparation stages, as well as intrinsic toxicity or elemental shortage. Furthermore, the applicability of lasting luminous nanoparticles photovoltaic cells, biomedical scanning and identification, and safety encryption has piqued interest. Moreover, we discuss the production, characteristics, the uses of luminescent substances, as well as the problems and future of these substances. Lastly,

***K E Y W O R D S***

*COVID-19, risk factor and Kabul city*

| | |
|---|---|
| from the standpoint of the synthesis, several additional suggestions have been made to improve its luminescence responsiveness. One such study, we expect, will hasten overall synthesis of SrAl2O4-based nanomaterials. | |

## Introduction

This study's objective, which is based on a previously published work, is to describe recent developments, particularly in the synthesis of luminescent nanoparticles. We cover recent developments on SrAl2O4: Eu, Dy nanoparticles in highlighting the advantages and drawbacks of various fabrication techniques. Upon absorption of energy from a source of radiation, phosphors materials emit light [6]. Such substances may possible be classified in a number of different means, like chemical family, usage, and even stimulation source. Based upon how well they are aroused, they are classed as photoluminescence, cathodoluminescence, triboluminescence, sonoluminescence, electroluminescence, thermoluminescence, chemiluminescence, and bioluminescence. Conjugated polymers, organic paints, transition metals, semi - conductor, and synthetic luminescence forms a small fraction of the dazzling compounds that have been developed for varied applications. Despite the advancements made, improving their optical properties remains a difficulty. The majority of phosphors are manmade. Organic luminous compounds, on the other hand, have recently received a lot of attention. In this section, we'll look at artificial photoluminescence [7].The following paper will go over some inorganic phosphor production methods, with an emphasis on enhanced synthesis procedures for Strontium monoaluminate based nanomaterials, and the relationship amongst microstructure and luminescence response. Luminescence mechanism [5]. The second section focuses on laboratory preparation of SrAl2O4-nanopoweders, encompassing everything from traditional to modern fabrication techniques like hydrothermal, CPT, micro emulsion and thermal processes spent a lot of time and effort creating new methods for obtaining sub–micrometric particles that eliminate onerous, complex, time-consuming, expensive, or inefficient preparation phases, as well as inherent toxicity or component scarcity[8]. This is important to note that, utilizing an innovative molten salt synthesis technique, we previously revealed a substantial luminescence sensitivity for SrAl2O4 -based nanomaterials with sub–micrometer particle size[9].

## Experimental

### Materials

Sr(NO3)2 bought from Jihan Chemicals Ltd , China; aluminum nitrate , europium nitrate and dysprosium nitrate purchased from the same company have been used as building ingredients, along with a small portion of boric acid as a flux. With no more purification, all of the substances were used as obtained. Throughout the synthesis process, distilled water was used.

### Fabrication Process

To make chemical materials, the alkaline aluminates and dissolved salts nitrates were Main ingredient that were blended in a stoichiometric mixture of Sr0.95Al2O4: Eu0.02, Dy0.03. As a flux, 5% boric acid was added. A quantity bead loading of 60% was used. 1500rpm was the angular velocity utilized [10]. This same high-energy density stirred media mill was used to extensively grind the compositions for different periods of time (i.e., 0, 20, 60, 120, and 180 minutes). For powdered form constituents,

the mechanochemically pretreated mixture was left to dry in the oven for a day at around 60°C and manual operation process in an agate mortar[11]. Furthermore, as a known luminescent nanomaterial the byproduct blend that has not been in the mill was first blended to alcohol in a molar ratio of 1.01.6 for 20 minutes under magnetic stirring, after that it was left to dry then crashed to powdery form manually. To finalize the fabrication process mixtures were moved into crucibles and heated in an electrical furnace in a reducing environment for 3 hours at a different temperature (800,900, 1000, 1100, 1200, 1300, and 1400°C). At last, most of the pre-heated nanomaterial powders are left to cool down before being physically milled to powdery state for about half an hour and filtered to obtain the establish positive. SrAl2O4: Eu2+, Dy3+ powder.

**Characterisation**

A laser diffraction particle diameter analysis software was used to examine the crystallite size pattern of the powdered [10]. XRD was used to measure the crystal structures of the powder materials. SEM was used to examine the geometry as well as appearance of the particles formed .FTIR was used to collect the particles FTIR spectra in the spectral region of 400–4000cm-1. The PL excitation and emission spectra, as well as the time-resolution photoluminescence spectrum, were also collected. In such a dim environment, the ML characteristics at various pressure pressures and periods were tested using an impact method in a specially developed ML measuring system [12]. By turning off the UV, physical tension has been administered after the particular amount of time had passed. This ML subsequently abruptly stimulated so use a process where a 0.1kg force had been thrown out of a distance onto the luminescent surface via a directing tube. The ML measurement device allows a storing recorder to concurrently exhibit physical stimulation and ML information in actual time. Following the implementation of noise reduction and electrical insulation on the test apparatus, a greater demodulation ratio was achieved. A greater signal-to-noise ratio with vivid report pulses had been generated by implementing a variety of techniques like sound insulation and electrical insulation on the research apparatus[13].

**Results and Discussion**

The effect of grindability on particle diameter in basic ingredients as well as precursors mixes [14]. Its average particles of SrCO3 and Al2O3 are shown in the graphs below there are between, at 4.521± 0.006 nm and 15.417± 0.013 nm. High-energy milling is, in fact, nothing more than an energy transfer process. Because of splitting and compressing processes in the crystals, momentum for particle fracturing moves across crystals to parent particles during processing. The particles of precursors break when mechanical energy from beads is applied to them, and their particle sizes decrease as a result [15]. As a result, grinding time influences the extent of particle size reduction units average grain size and morphology of the unprocessed and processed precursors solutions at various times. These findings suggest that milling efficiency can be improved early in the process. Because there are fewer flaws and tiny particle clumping when milling for a longer period of time, the milling efficiency suffers

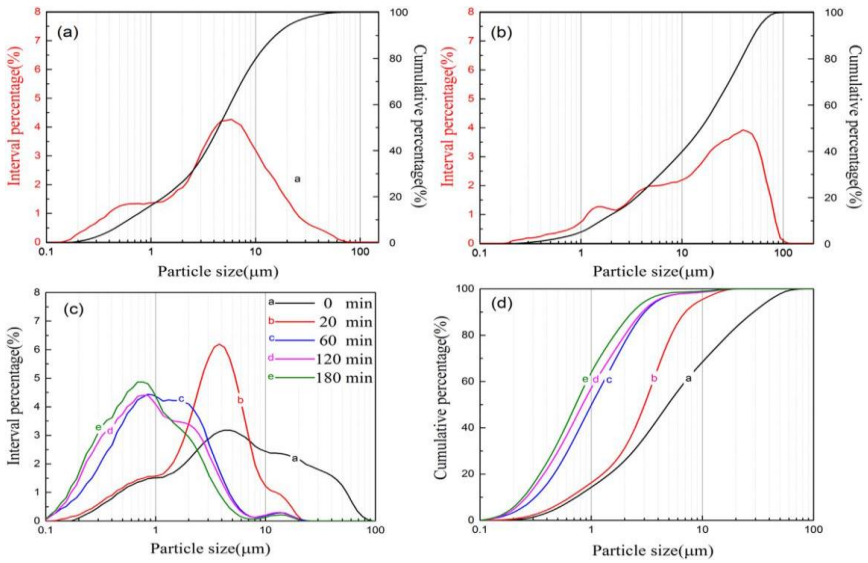


Figure: particle size distributions of the main raw materials and precursor mixtures (a) srco3, (b) al2o3, (c) and (d) precursor mixtures unground and ground pretreated at different durations..

SEM micrographs of unprocessed and processed precursor mixes at various times. For the unground precursor mixture, (a), there are different particles with two characteristics. The larger nanoparticles are mostly SrCO3, which is recognized by the (See . (f) for an EDX2 spectrum.)

Table : Median size and specific surface area for precursor mixtures unground and ground at different durations.

| **Grinding duration, min** | **0** | **20** | **60** | **120** | **180** |
|---|---|---|---|---|---|
| **Median size, μm** | **5.451 ± 0.016** | **3.367 ± 0.007** | **1.124 ± 0.012** | **0.929 ± 0.004** | **0.808 ± 0.007** |
| **Specific surface area, m2/g** | **1.52 ± 0.08** | **7.31 ± 0.06** | **17.35 ± 0.03** | **26.48 ± 0.04** | **31.50 ± 0.06** |

The EDX1 spectrum identifies those blocky nanoparticles as Al2O3. As the crushing time goes on, the size of the nanoparticles shrinks and the mixture's uniformity improves. Subsurface specimen can break due to bruising and compacting forces (i.e., alumina beads). The nanocrystals are often evenly distributed, as seen in Fig. (c), and the decreased particle size at 1 hour is less than 1.5 μm. As a matter of fact, it's assumed that tiny, uniformly spaced particles could aid in the subsequent process's cooling. Spectra of unglazed ceramic and ground precursor mixtures over period are depicted in . (a). The data's properties clearly show that SrCO3, Al2O3, Eu2O3, and Dy2O3 exist. The scattering concentration decreases and the ½ width widen as the milling time is increased, implying that the crystallinities of the precursor nanoparticle in blends decline and even amorphize.

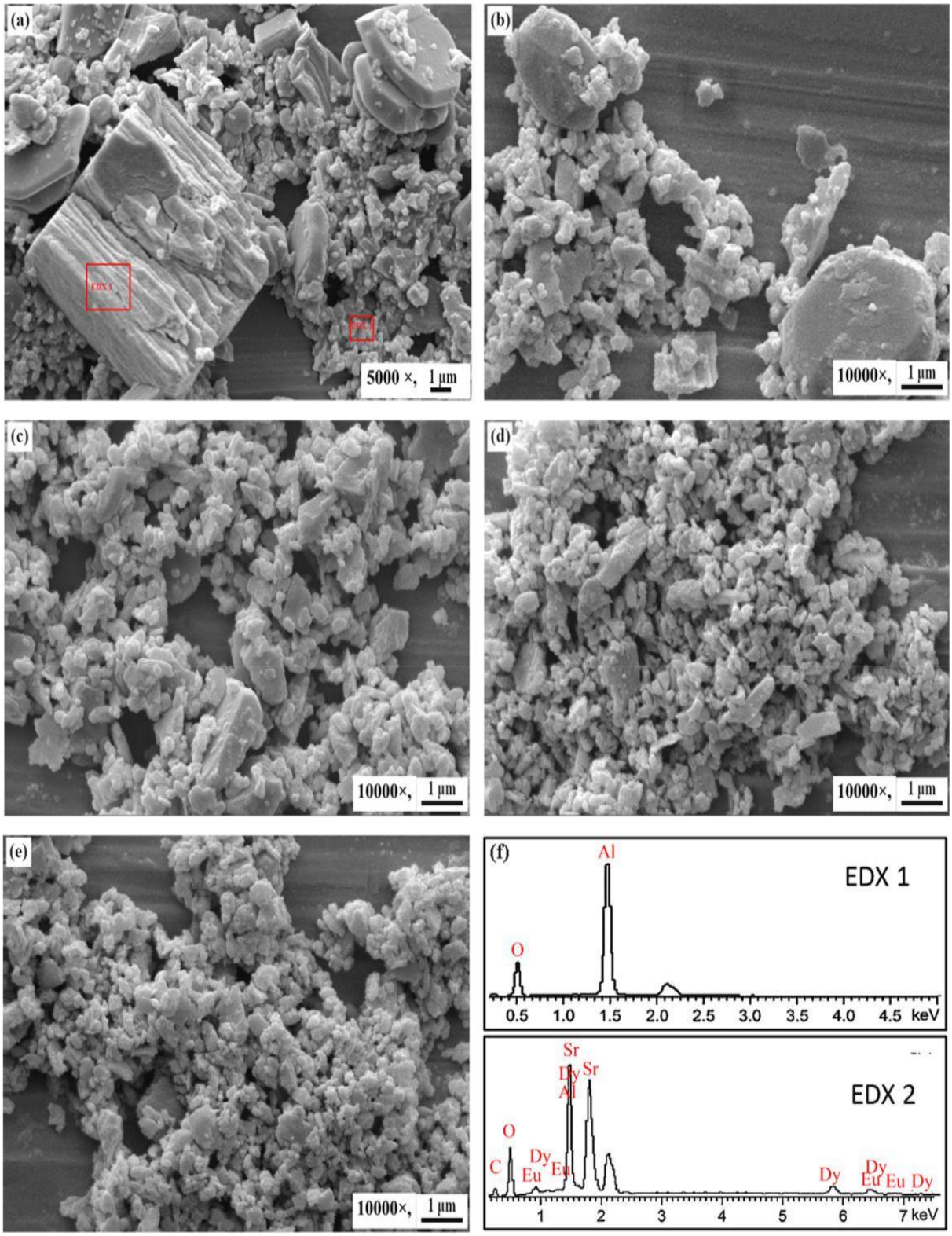


Figure: The SEM images of precursor mixtures unground and ground at different durations. (a) 0 min, (b) 20 min, (c) 60 min, (d) 120 min, and (e) 180 min, (f) the EDX analysis of the unground precursor mixture

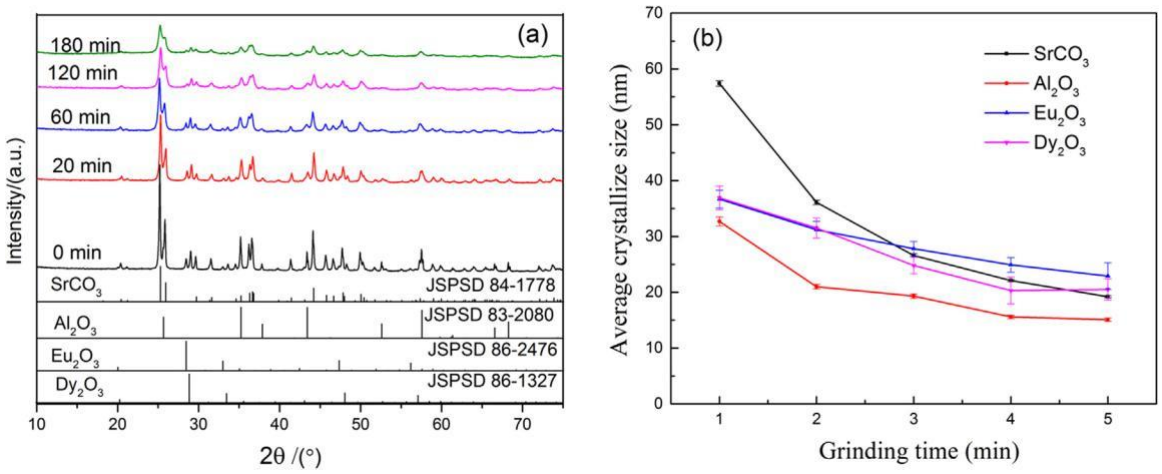


Figure: The XRD patterns and average crystalline size of precursor mixture unground abd ground at different durations.

Demonstrates the FTIR spectrum of precursor mixtures ground at 400–4000 cm for 0 minutes, 60 minutes, and 180 minutes. The absorption peaks are caused by excitations in CO32- at 400–1800 cm Consequently the reduced vibratory clusters, the brightness of the maxima at 1474, 1071, and 855 cm reduce, and the reached its maximum at 703 cm vanishes as the milling period grows.. Furthermore, this same characteristic peaks' stretching vibrations.

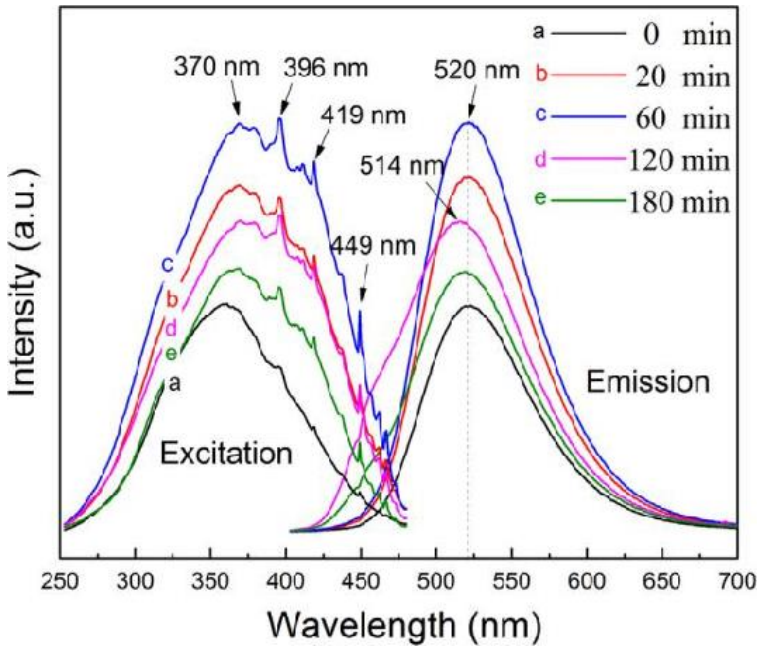


Figure**: Photoluminescent excitation and emission spectra of SrAl2O4: Eu2+,Dy3+ phosphor synthesized with the precursor mixtures unground and groundat different durations and calcined at 1200 °C**

Absorption spectra magnitudes of luminescence manufactured with processed precursors are higher than either luminescence produced with unprocessed constituents. Definitely, doping can improve phosphor's photoluminescence characteristics. The luminescence produced by grinding the precursor mixture for 60 minutes has the maximum emission spectra. At the right ratio, Eu2+ and Dy3+ ions have a synergistic impact, as is. When nanomaterials are made with stoichiometric amounts of

Sr0.95Al2O4: Eu0.02, Dy0.03, there is no photoluminescence intensity. Larger quantities of the rare earth ions dissolved into SrAl2O4 nanomaterial, more phosphors center levels and trap levels occur, resulting in higher PL and ML intensities. Since the tensile load on the precursor particulate aims at promoting the doping of Eu2+/ Dy3+ charged particles into SrAl2O4, the quantity of Eu2+/ Dy3+ charged particles disintegrating into SrAl2O4 grows at a suitable grindability .

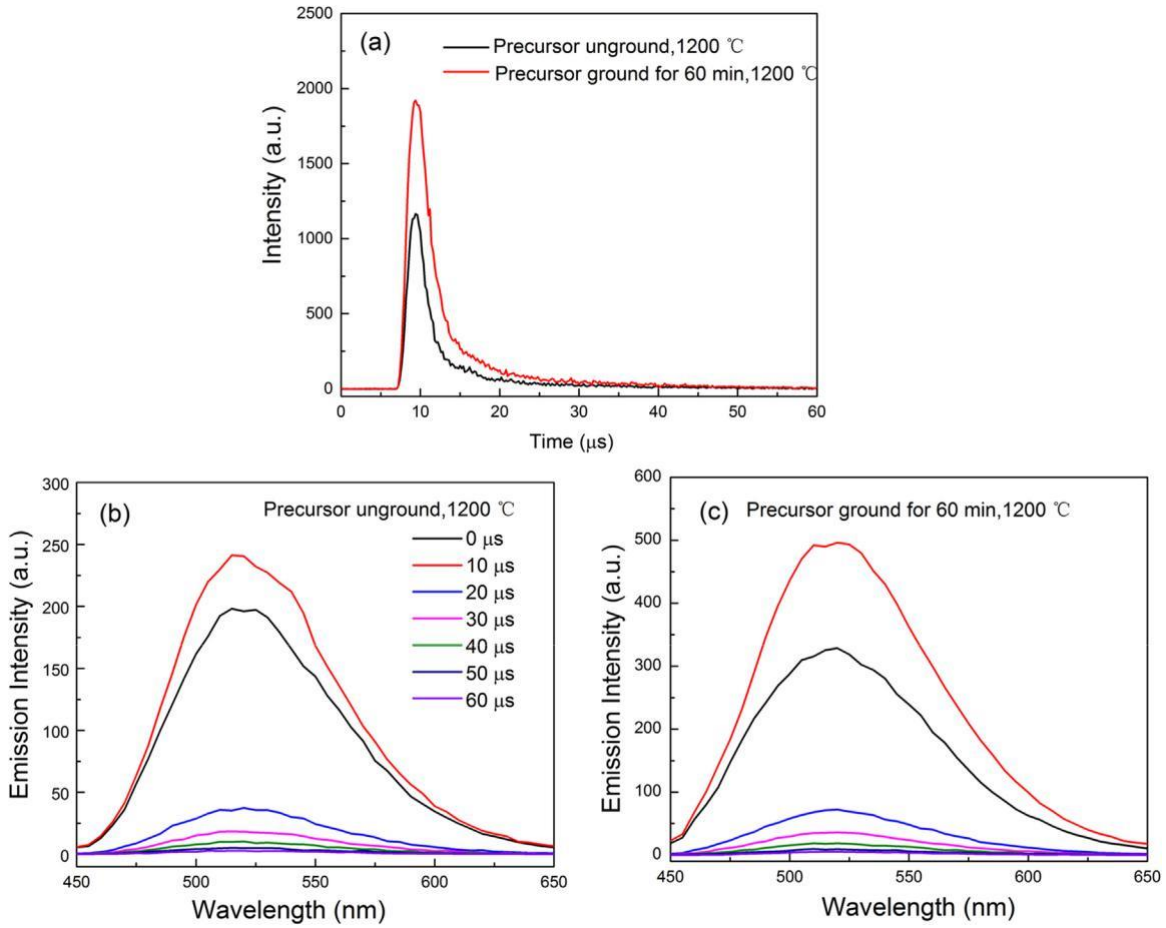


Figure**: Time-resolution photoluminescence spectra of SrAl2O4: Eu2+, Dy3+ phosphor synthesized with the precursor mixtures unground and ground for 60 min and calcined at 1200 °C. The collected time range is from 0 to 60 μs.[1]**

SrAl2O4: luminescence spectra with time resolution: Eu2+, Dy3+ phosphor was manufactured using unground precursor mixtures that were ground for 60 minutes before being calcined at 1200 °C. To understand more brightness decline and compare spectra, we had to use a timeframe luminescence range evaluation for SrAl2O4:Eu2+,Dy3+ nanomaterials had been prepared with unground and ground precursor mixtures for 1 hour and calcined at 1200 °C. The luminance degradation and output peak was observed of photoluminescence samples were investigated for 520 nm emission under 370 nm wavelengths. The time gap of 0-60 minutes at a time was acquired. An absorption edge of photoluminescence nanoparticles were prepared with 1 hour ground precursor combinations is obviously higher under UV activation. A significant correlation is seen in the brightness decay. As per period PLemission spectra, there is also an output center in SrAl2O4:Eu2+,Dy3+ nanomaterial, and

Eu2+ has an emission spectrum peak at 520The strength goes up and afterwards ends up falling with the delay, attaining its highest at t = 10 s.

Figure below depicts the tension procedure used in the scheduled ML model simulation (a). When a mass of 0.1 kg is dropped from some length (i.e., 5, 10, 15, 20, 25, and 30 cm), the implications pressure produced on the brightness disk greatly increases, exhibiting the designed state's highest sensitivity and ability to respond. 1 nanosecond is the length of time. The numeric persistence of standard safety-related assessment different at various peaks from Eq. (1) is 10.39, 14.65, 17.92, 20.68, 23.11, and 25.31 MPa, which are similar to results obtained using a computer memory oscilloscope.

The up a nationwide pressure on a luminescent disk at the same delay time. The photoluminescence disk is produced of particles epoxy polymer and SrAl2O4:Eu2+,Dy3+ phosphor, which was produced using a 60-minute grind of the precursor mixture. The implications pressure of the luminescent disk is specifically related to the ML brightness. When the strain is completely filled, the ML signal appears, and the ML intensity grows as the implications pressure builds. According to Bünzli et al. and Canadra et al., the ML emergence of phosphorescence is associated with piezo-electrification. The use of stability applications causes a highly centralized piezoelectric field in SrAl2O4:Eu2+,Dy3+ crystals, lowering the trap depth. The freed molecules enter the band gap and transfer their energy to the inducer Eu2+

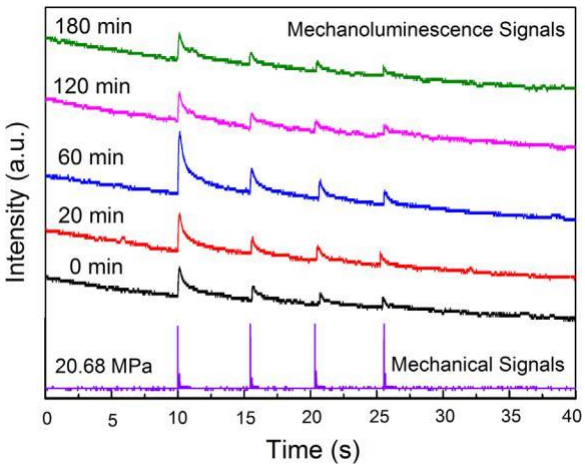


Figure : ML intensity of SrAl2O4: Eu2+, Dy3+ phosphor disks prepared with the precursors mixture unground and ground at different durations and calcined at 1200 $^0$C

ML intensity of SrAl2O4: Eu2+, Dy3+ nanoparticles prepared for varying lengths of time with such a combination of unground and ground byproducts and calcined at 1200 °C . Ions are responsible for its luminescence. A photoluminescence disk with a greater range tension may have a narrower trap width. More and more trapped ionized particles that can be released immediately, the brighter SrAl2O4 becomes: Eu2+, Dy3+. Fig. depicts the ML brightness of SrAl2O4:Eu2+,Dy3+ phosphor disks prepared with unground and ground precursor mixtures for various times[16]. The ML mechanism is evidently caused by numerous uses of exactly equivalent impact stresses on each phosphor disk simultaneously slope of delay curves. Furthermore, the ML intensity decreases when multiple equal impact stresses are applied to the same phosphor disk. Canadra et al. also reported similar results.

Moreover, when particularly in comparison to luminescent nanomaterial synthesised with unground and ground byproduct mixtures for longer periods of time (i.e. > 1 hour), the phosphor disk prepared with the precursor mixture ground at 1 hour has the highest ML intensity[17]. The ML concentration

and the PL concentration are considered to be linked. As aforementioned, the brightness produced with the byproduct combination ground for 1 hour has the greatest Pl spectra. When the luminous disk, which has been ground for 60 minutes with the precursor combination, is exposed to UV light, more electrons are trapped and stored in traps. A comparable decreasing trend in trap level of detail could be achieved by utilizing the same forces acting to a phosphor disk. As a result, more detrapped electrons may enter conductive bands and be gathered in the excited state of Eu2+ ions, resulting in stronger luminescence. As a consequence, an unplanned connection exists among soft and hard.

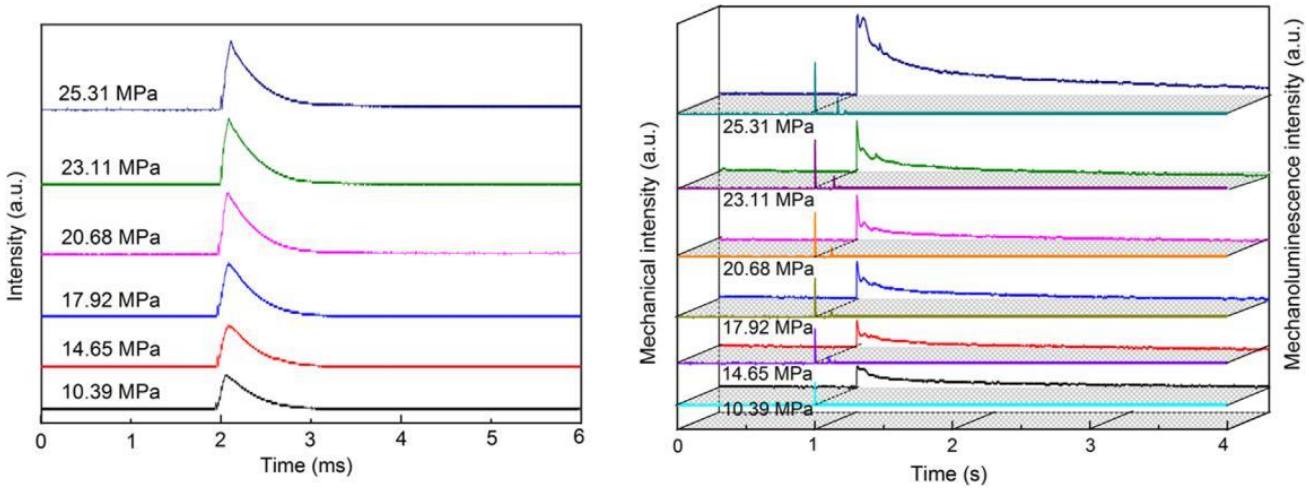


**Figure: mechanical stress and mechanoluminescence signals. (a) the sensitivity analysis on mechanical stress for the designed ml measurement system. (b) ML intensities of phosphor disk prepared with the precursor mixture ground at 60 min induced by the mounting impact stress at the same delay time**

Figure: mechanical stress and mechanoluminescence signals. (a) the sensitivity analysis on mechanical stress for the designed ml measurement system. (b) ML intensities of phosphor disk prepared with the precursor mixture ground at 60 min induced by the mounting impact stress at the same delay time

## Conclusions

SrAl2O4 doped with rare earth ions for this case europium and dysprosium nanoparticles were prepared, followed by heated treatment in a reduced atmospheric conditions for a brief span of time. Soft mechanochemical purification of precursor compositions reduced median crystallite sizes, enhanced uniformity and morphology of the byproduct, doubling the reaction of the byproduct, advantaged particle activity and reducing the crystal growth time and following heating temperature for SrAl2O4:Eu2+,Dy3+. According to DSC analysis, the crystal growth temperature and time of SrAl2O4 could be reduced to 1144 °C and 18.2 min then crushed to powdery form for about one hour. Furthermore, this same activation energies of SrAl2O4 calculated for the crushed and uncrushed unground for one hour byproduct compositions, were 839.8 and 659.7 Kj/mol, suggesting that which was before might lower the kinetic energy of crystal growth of SrAl2O4, resulting in a lower sinter-crystallization temperature. Moreover, for the luminescence of SrAl2O4:Eu2+,Dy3+ phosphor, a disturbance band appears over a wideband, with a significant emission spectrum at 520 nm[3]. A crafted analyzer with a good precision and responsiveness was used to observe the mechanoluminescent property of a reactive polymers combined with prepared nanoparticles SrAl2O4.

The instrument allows a spectrum analyzer for storing data to simultaneously show physical perturbation impulses and machine learning indicators.

**References**

1. R. Zhou, F. Ma, Y. Yang, T. Deng, J. Li, H. Zhao, J. Sheng, Q. Peng, Enhanced thermal stability and afterglow performance in Sr 2 Ga 2− x Al x SiO 7: Ce 3+ phosphors via band gap tailoring, Inorganic Chemistry Frontiers, 9 (2022) 23-34.
2. J.J. Ahn, Y. Kim, E.A. Corley, D.A. Scheufele, Laboratory safety and nanotechnology workers: an analysis of current guidelines in the USA, NanoEthics, 10 (2016) 5-23.
3. R. Cao, X. Wang, X. Ouyang, Y. Jiao, Y. Li, H. Wan, W. Li, Z. Luo, Thermally stable orange-red emitting Ba2SiO4: Sm3+ phosphor: Synthesis and luminescence properties, Journal of Luminescence, 224 (2020) 117292.
4. C.V. Devulkar, Inculcating Values and Ethics among Students through Steam Education, International Journal of Multidisciplinary Research and Explorer (IJMRE) May-2021, (2021).
5. Y. Furuhata, A. Sakai, T. Murakami, A. Nagasaki, Y. Kato, Bioluminescent imaging of Arabidopsis thaliana using an enhanced Nano-lantern luminescence reporter system, PloS one, 15 (2020) e0227477.
6. Z. Ni, T. Fan, S. Bai, S. Zhou, Y. Lv, Y. Ni, B. Xu, Effect of the Concentration of SrAl2O4: Eu2+ and Dy3+ (SAO) on Characteristics and Properties of Environment-Friendly Long-Persistent Luminescence Composites from Polylactic Acid and SAO, Scanning, 2021 (2021).
7. Y. Kim, J. Park, M. Park, Creating a culture of prevention in occupational safety and health practice, Safety and health at work, 7 (2016) 89-96.
8. R. Hu, Y. Zhang, Y. Zhao, X. Wang, G. Li, C. Wang, UV–Vis-NIR broadband-photostimulated luminescence of LiTaO3: Bi3+ long-persistent phosphor and the optical storage properties, Chemical Engineering Journal, 392 (2020) 124807.
9. A.N. Bone, Optimization of a Strontium Aluminate, in, Oak Ridge National Lab.(ORNL), Oak Ridge, TN (United States), 2017.
10. J. Sort, Nanocomposite Materials: A Section of Nanomaterials, in, Multidisciplinary Digital Publishing Institute, 2022, pp. 203.
11. K. Song, H. Yu, Q. Nie, Y. Bai, Y. Guan, J. Yu, L. Guo, Synthesis and luminescence characteristics of Mg2Al4Si5O18: Eu2+ and nitrided Mg2Al4Si5O18: Eu2+ phosphors, Journal of Luminescence, 224 (2020) 117317.
12. X. Tang, E.D. Ehler, E. Brost, D.C. Mathew, Evaluation of SrAl2O4: Eu, Dy phosphor for potential applications in thermoluminescent dosimetry, Journal of Applied Clinical Medical Physics, (2021).
13. J. Wang, B. Liu, W. Chen, Q. Qiang, L. Peng, T. Han, T. Zeng, Z. Zhou, Z. Yang, Y.A. Nikolaevich, Variable temperature persistent luminescence properties of phosphors with continuous traps, Journal of Luminescence, 243 (2022) 118644.
14. W. Wang, A. Sha, Z. Lu, M. Jia, W. Jiang, Z. Liu, D. Yuan, Self-luminescent cement-based composite materials: properties and mechanisms, Construction and Building Materials, 269 (2021) 121267.
15. Y. Wang, P. Feng, S. Ding, S. Tian, Y. Wang, A promising route for developing yellow long persistent luminescence and mechanoluminescence in CaGa 2 O 4: Pr 3+, Li+, Inorganic Chemistry Frontiers, 8 (2021) 3748-3759.

16. C.H. Yen, R. Cheong, Application of Green Solvents for Rare Earth Element Recovery from Aluminate Phosphors, Minerals, 11 (2021) 287.
17. S.-K. Sun, H.-F. Wang, X.-P. Yan, Engineering persistent luminescence nanoparticles for biological applications: from biosensing/bioimaging to theranostics, Accounts of chemical research, 51 (2018) 1131-1143.